Pulse Shape Measurement Using Golay Detector

A. K. Kaveev, E. G. Kaveeva & E. A. Adaev

Journal of Infrared, Millimeter, and Terahertz Waves

ISSN 1866-6892
Volume 33
Number 3

J Infrared Milli Terahz Waves (2012)
33:306-318
DOI 10.1007/s10762-012-9879-9

Springer

J Infrared Milli Terahz Waves (2012) 33:306–318
DOI 10.1007/s10762-012-9879-9

Pulse Shape Measurement Using Golay Detector

A. K. Kaveev · E. G. Kaveeva · E. A. Adaev

Received: 2 December 2011 / Accepted: 2 February 2012 /
Published online: 28 February 2012

Abstract The article discusses key physical processes within the active area of an opto-acoustic detector. Said area is a xenon-filled chamber subdivided into two cavities connected by a narrow channel. Original mathematical model of such area is proposed on the basis of thermodynamic processes that occur within. A method has been developed to measure a shape of a periodic pulse exceeding 0.5 ms duration at repetition rates ranging from zero to several hundred Hz. The measurement requires knowledge of a set of parameters describing a specific instrument. Principal points of detector calibration are discussed in brief.

Keywords Golay cell · Pulse shape measurement

1 Introduction

Photo-acoustic spectroscopy of gases and solid phases, possibility of that was discovered by Bell, was developed by Rosencwaig and others in 1980-th [1–6]. Also photo-acoustic imaging was developed [7]. Very good review of photo-acoustic devices in appliance to spectroscopy one may find in PhD thesis of Kavaya [8]. Some works (for example, [4, 8–10]) were devoted to mathematical model of photo-acoustic detector development. Nevertheless, nobody has applied any such method to Golay cell. The constructions of photo-acoustic detectors (OADs) used in spectroscopy imply relatively large (in compare to Golay cell) gas chamber where pressure (i.e. acoustic) waves propagate and resonant properties of the gas are important because of spectroscopic application for example, [11] in contrast to Golay cell. Model of Rosengren implies pressure front calculation from close to rectangular input pulse series, in approach of constant gas concentration, and taking into account resonant properties of the pressure wave. The problem of calculation of input wave from known pressure change was not solved. Also variations of gas density (that is critical for Golay cell behavior description) were not implied.

A. K. Kaveev (✉) · E. A. Adaev
Tydex J. S. Co., 16 Domostroitelnaya str., 194292 St. Petersburg, Russia
e-mail: andreykaveev@tydex.ru

E. G. Kaveeva
St.Petersburg State Polytechnical University, 29 Polytechnicheskaya str., 195251 St.Petersburg, Russia

Apart of gas-based opto-acoustic detectors there are other types of OADs. For example, high power THz and RF opto-acoustic detector based on liquid state [12] was developed in last years. Nevertheless, in all cases opto- (or photo-) acoustic method of measurement is based on the same principle: transformation of optical wave into acoustic one and detection of the last.

Golay cell is based on a design first introduced by M. J. E. Golay in 1947 [13, 14]. Key features that enable efficient usage of the detector in various applications include its small size, operability at room temperature, high sensitivity, high efficiency and wide operating wavelength range. The device is a non-selective uncooled detector (see Fig. 1). Most prominent fields of application of the detector include characterization of IR sources and receivers [15], monitoring of IR radiation fields [16], measurement of weak IR fluxes for spectrometry and low-temperature pyrometry applications [17], metrology [15, 18], and various scientific applications that require detection of low-level signals (up to 10^{-5} J) in the wavelength range from 15 μm to 6–8 mm [17].

Principle of operation of the detector is as follows. Incident radiation falls on elastic absorbing film. Due to heat transfer, xenon in the cavity between the entrance window and the reflecting film is heated. Temperature in the cavity increases leading to change of pressure and bowing of the reflecting film. Position of a signal reflected by the film, i.e. its magnitude change after passing through the raster, is measured by a photodiode. Signal measured by the photodiode is transmitted to a recorder (such as oscilloscope). Volume of the cavity (V) described above is just a small part of total volume of the xenon-filled chamber. Small cavity is connected to larger volume by a narrow channel allowing to equalize xenon density and pressure.

This detector has been conventionally used to measure power of continuous signals. It requires interruption of the measured flux by an optical modulator. In this article, we for the first time present the possibility to use optoacoustic detector (OAD) for measurement of periodic signals of arbitrary shape, and single pulses. This allows one to measure not just pulse magnitude, but also its shape, i.e. power as a function of time, $p(t)$. Thus, optoacoustic detector's area of application can be substantially extended. Such type of measurement is

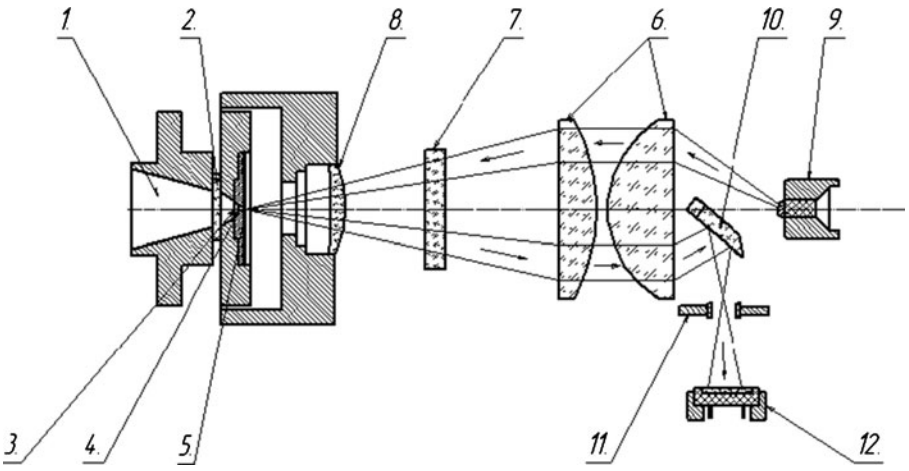

Fig. 1 Golay cell schematics. 1 – cone, 2 – window, 3 – absorbing film, 4 – channel, 5 – membrane, 6 – condenser, 7 – raster, 8 – objective lens, 9 – LED, 10 – mirror, 11 – diaphragm, 12 – photodiode.

made possible by application of the mathematical model of the OAD presented in this article. Any signal amplitudes that may be detected by the OAD can be used for calculations. Pulse recurrence rate can range from zero to several hundred Hz. Single pulse duration should be at least 0.5 ms (possible cause of this limitation is discussed later). Pulses must be separated by intervals of constant incident power (zero for example). There are no limitations on duration of those intervals. Moreover, the energy per pulse for ultra-short impulses (with duration about nano-, picoseconds *etc*) may be calculated. The technique was tested and approved in Tydex J. S. Co.

The common opinion is that Golay cell may be applied strongly to continuous modulated signals. We suggest in our paper to broaden the range of Golay cell applications to some that previously were considered not applicable to this device. For example, Golay cell may be applicable for power and pulse shape calibration of pulsed (including ultra-short) IR lasers with pulse repetition rate about 1 kHz and less. Also, the measurements of pulse characteristics of Cs-based gas-discharge lamps [19] are actual to date. Apart, we may speak about general scientific task of single IR pulse analysis. Even if the pulse duration is shorter than 0.5 ms, with use of Golay detector we may calculate the power per pulse, without pulse shape measurement. All these applications drastically increase the possibilities of Golay cell use. Furthermore, even in "usual" cases of continuous modulated signal, if the aperture of the source (i.e. black body) is comparable to the area of optic knife, calculations that occur without corrections related to considered mathematical model, may contain the mistakes till 10-20%.

2 Mathematical model description

The presented mathematical model is based on thermodynamic representation of active area of the instrument. According to this model, the device can be described using a standard set of thermodynamic parameters (see Fig. 2). Here, P and P_0 are xenon pressure within the cavity volume V constrained by absorbing and reflecting films, and within the bigger chamber, respectively. T and T_0 are the respective xenon temperatures within the aforementioned volumes, whereas n is the xenon density in volume V.

The cavity V is not completely pressurized. Instead, it's connected to larger chamber volume with a narrow channel. Absorbing film is heated by incident energy flux $p(t)$, which we need to reconstruct. Detector outputs time-dependent response signal $U(t)$ which is recorded, e. g. using an oscilloscope.

It is shown that in fact two different mathematical models are better suited for the repetition rates of the measured signal above and below 6 Hz, respectively. Let us discuss both of these cases.

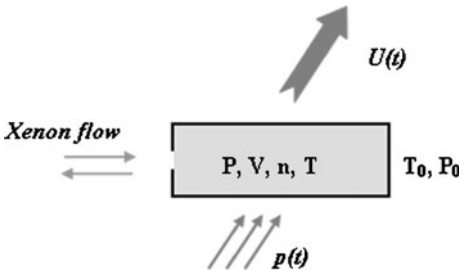

Fig. 2 Simple model of active area of OAD.

2.1 Repetition rates of 6 Hz and above

The active area (cavity) of the OAD can be described with the following equation:

$$\frac{3knV}{2}\frac{dT}{dt} = p(t) - \frac{3}{2}knV\frac{T - T_0}{\tau_T}. \quad (1)$$

Here, τ_T is a cavity parameter with a meaning of "instrument response" that describes cooling of the volume V. All other parameters are as described above. This equation describes heat balance in active cavity volume. Left part of the equation is the change of energy of the active volume, whereas right part is the difference between heat inflow from external source (1st term in r.h.s.) and heat outflow due to cooling (2nd term in r.h.s.). At repetition rates above 6 Hz, variation of xenon density within the active volume is negligible, i. e. $n(t) \approx const$.

The Eq. (1) implies that

$$p(t) = ck\left(\frac{dT(t)}{dt} + \frac{T(t)}{\tau_T}\right) + base,$$

but more precise approximation of the desired signal may be achieved by introducing second-order correction:

$$p(t) = c\left(\frac{md^2U(t)}{dt^2} + \frac{dU(t)}{dt} + \frac{U(t)}{\tau_T}\right) + base, \quad (2)$$

where constant m describes corrections due to resonance characteristics of the system, and c in (2) describes the magnitude of the incident signal. Equation (2) is based on assertion $U(t) \sim P(t) \sim T(t)$. The constant value *base* is necessary to normalize the Eq. (2) to constant (background) incident power (zero for example). Hence, the parameters τ_T, m and c are instrument-specific and may be determined by calibrating the OAD. Sign of the constant c is also dependent on specific OAD.

Let's describe the procedure of determining the aforementioned parameters. To determine the constant τ_T, one needs a pulse source with constant incident power intervals. Precise amplitude of the pulses may be unknown. The simplest case is a meander signal, i. e. a sequence of rectangular pulses. One of the possible ways to generate such a signal is a pulsed mode LED. Continuous mode LED with optical modulator yields even better results. Experimental geometry must provide lowest possible time of partial aperture closure with a shutter. The better this condition is satisfied, the closer to meander is the pulse shape. Pulse generator may be used instead. Figure 3 depicts generic response of OAD to such signal as a function of time.

Response period is equal to incident signal period; ascending regions correspond to heating of the active area, whereas descending regions correspond to cooling (i. e. constant or zero incident power). τ_T may be estimated from $\exp(-\frac{U(t)+B}{\tau_T}) - D$ by fitting the parameters of this exponent to the calibration curve describing the chamber cooling.

To evaluate the parameters m and c, voltage-power characteristic of the OAD may be used. This characteristic describes dependence of optical sensitivity of the detector (i. e. ratio of the output voltage of the detector to the incident signal power) on the signal repetition rate. To obtain this characteristic, modulated continuous source of known power output (such as black body) is used.

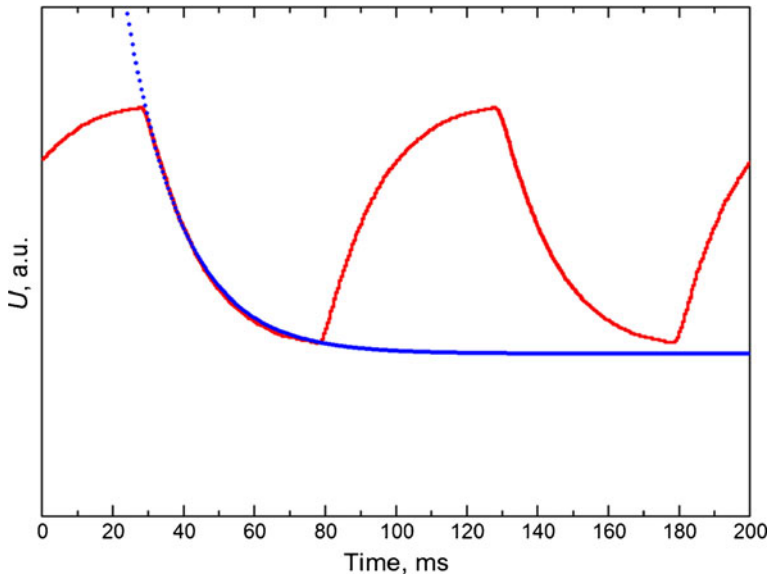

Fig. 3 OAD response to a sequence of rectangular pulses (calibration curve). Exponential extrapolation of the region corresponding to constant incident power.

To evaluate the parameters, one may assume that in the case of aperture area comparable to shutter area, modulated black body signal can be closely approximated with sine wave. In the case of sine-wave *U(t)*, the Eq. (2) has the following exact solution:

$$\frac{U_{\max}}{p_{BB}} = \frac{1}{C\sqrt{(2\pi F)^2 + \left(\frac{1}{\tau} - m \cdot (2\pi F)^2\right)^2}}, \tag{3}$$

where F is the black body modulation frequency in the range of several Hz to several tens of Hz. Unknown parameters are determined by fitting the right part of Eq. (3) to the measured voltage-power characteristic of a specific OAD, see Fig. 4.

After that, these three parameters may be refined. Refinement is achieved using the responses to calibration signals. To adjust τ_T and m values, one may use the same rectangular pulse sequence with known duration and period that was used above to determine τ_T. The Eq. (2) is used to calculate power versus time *p(t)* for the pulse sequence; the parameters are varied to achieve best fit of the dependence. To adjust c value, reference black body signal of known power is used in similar way with modulation frequency 15–25 Hz.

Thus, after determining the set of parameters, we may obtain time dependence of power of the incident signal *p(t)*.

It should be noted that proper calculation of the time curve may require averaging measured response *U(t)* over several periods, as well as smoothing. These procedures are necessitated by significant noise in the reconstructed curve due to derivation of the response curve affected by random fluctuations. It should be also noted that the set of parameters must be determined at temperatures close to normal operating temperatures of the detector.

Figure 5 shows some samples of the signals calculated using the above method.

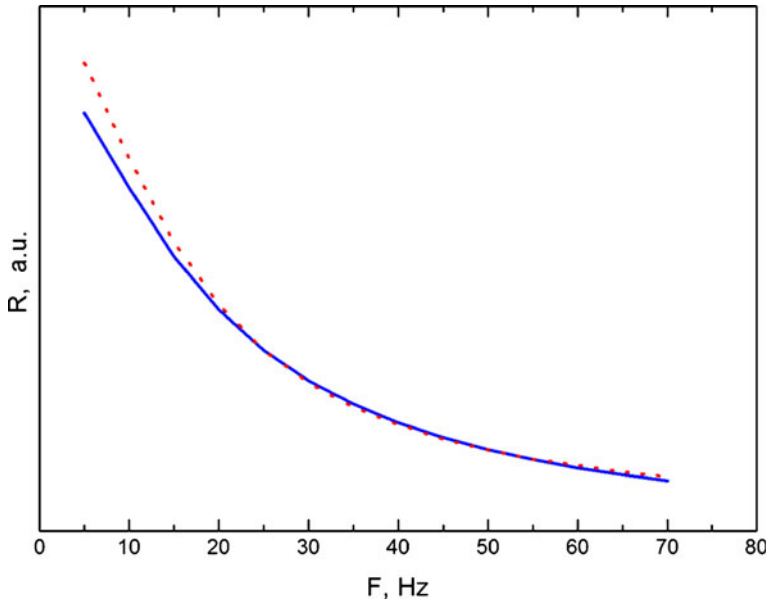

Fig. 4 Optical sensitivity vs signal repetition rate curve (dot) and its approximation (solid).

2.2 Repetition rates below 6 Hz and isolated pulse

In this case, greater characteristic times of the signals make slow processes significant. Therefore, time variations of xenon density in the active volume V due to particle exchange with larger chamber through connecting channel must be taken into account.

To describe this system, we must introduce another time parameter τ_P corresponding to the time of pressure equalization between sub-volumes of the chamber. Note that $\tau_P >> \tau_T$. Thus, besides Eq. (1), the active area of the OAD is described by the equation

$$V\frac{dn}{dt} = -\frac{V}{kT_0}\frac{P - P_0}{\tau_P}, \tag{4}$$

which is the equation of gas particle balance in the volume V. If we average this equation by time, and assume that time dependence of incident power $p(t)$ is periodic, we may conclude that $\left\langle \frac{dn(t)}{dt} \right\rangle = 0$, then $<P>=P_0$, and, therefore, time dependence of pressure in the cavity between the entrance window and the reflecting film is given by

$$P(t) = C(U(t) - \langle U(t)\rangle) + P_0 = CU(t) - \frac{C}{t_U}\int_0^{t_U} U(t)dt + P_0, \tag{5}$$

where t_U is a multiple of the period of incident signal. Therefore,

$$n(t) = n_0 - \int_0^t \frac{P(t) - P_0}{kT_0\tau_P}dt', \tag{6}$$

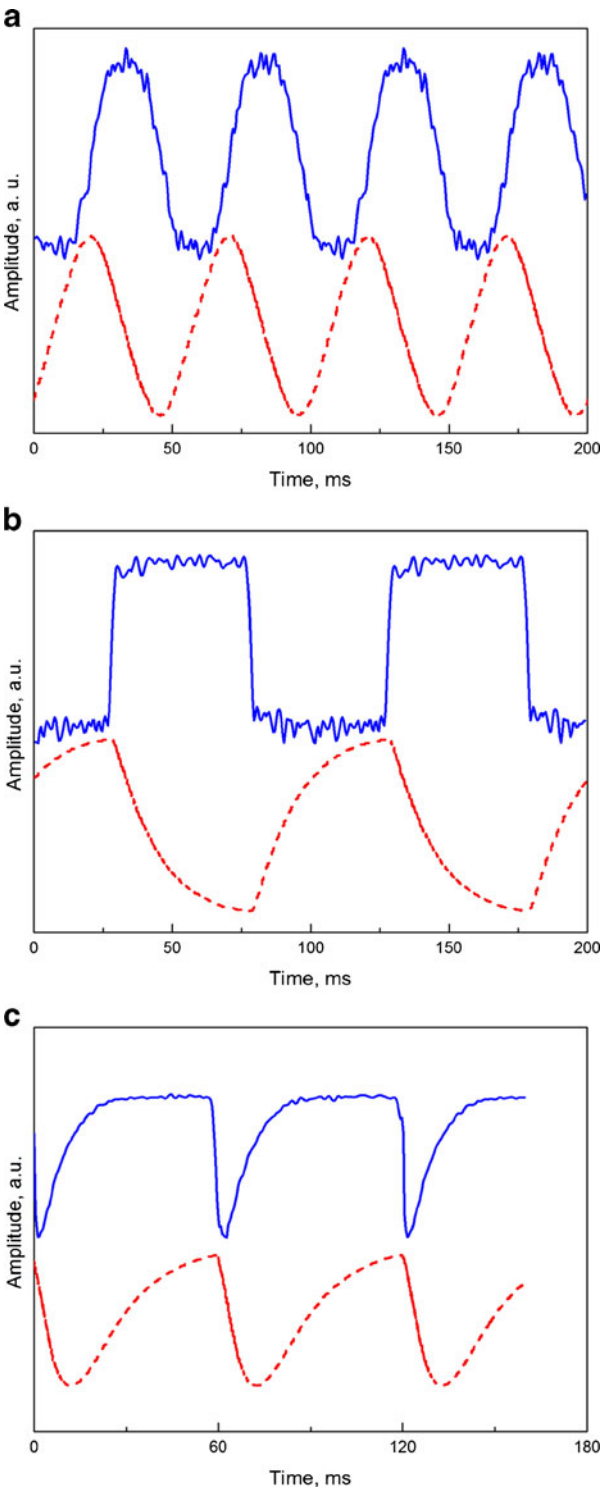

Fig. 5 OAD response vs time (dash) and corresponding calculated incident signal (solid). (**a**) – modulated black body signal with modulation frequency of 20 Hz; (**b**) – (50+50 ms) meander; (**c**) – sequence of asymmetric ("saw-tooth") pulses with frequency 20 Hz.

with n_0 dependent on choice of zero time. Assuming that pressure variation in the active volume is small compared to initial pressure, i. e. $P(t)\text{-}P_0 << P_0$, we may conclude that n_0 is close to average xenon density in the active volume, so that $n_0 = \frac{\alpha P_0}{kT_0}$, where $\alpha < 1$, $1-\alpha << 1$.

To summarize the aforesaid, reconstruction of time dependence of incident power $p(t)$ requires knowledge of four parameters: τ_T, τ_P, C and α. Note that the parameter C has somewhat different meaning than in the case of repetition rates above 6 Hz. This parameter describes dependency between $P(t)$ and $U(t)$ and is calculated in a different way. Fitting parameter α describes xenon density drop in the active volume V as compared to main chamber. Rather than being a device-specific constant, it is calculated individually for each $p(t)$ curve.

From Eqs. (1), (4) and from the equation $P(t) = nkT(t)$ one may conclude that

$$p(t) = \frac{3}{2} V \left(\frac{dP(t)}{dt} + \frac{P(t)}{nkT_0} \frac{P(t) - P_0}{\tau_P} + \frac{P(t) - n(t)kT_0}{\tau_T} \right). \tag{7}$$

Together with condition (6), this equation allows us to calculate incident power as a function of time. As in the previous case, the parameters τ_T, τ_P and C are determined by calibration of a specific instrument. Evaluation of the parameter τ_T is fully equivalent to the previous case. Evaluation of τ_P also requires a pulse source with regions of constant (or zero) incident power. However, pulse rate must be lower, namely about 1 Hz. The intent is to achieve the dependence $U(t)$ that includes the regions corresponding to equalization of xenon pressure between sub-volumes (see Fig. 6).

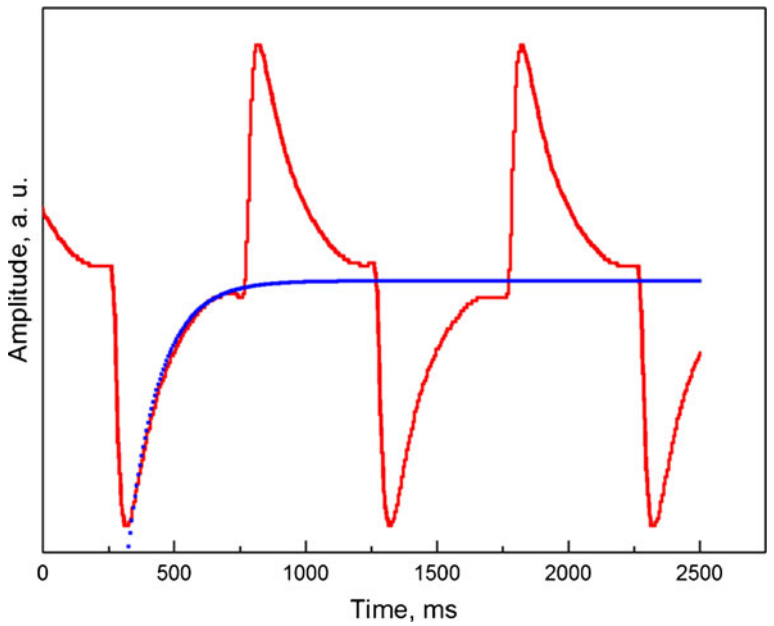

Fig. 6 OAD response to a sequence of rectangular pulses with a rate of 1 Hz. Sharp rises of the curve correspond to heating, gradual declines - to pressure equalization, sharp drops - to cooling, and gradual rises also - to pressure equalization (exponential extrapolation also shown).

Evaluation of the factor C in the pressure equation $P(t) = CU(t)$ is made in approximation $C \neq f(U)$. Let us take into account that at high repetition rates, i. e. $\frac{1}{F} << \tau_P$, xenon density in the cavity cannot change significantly. Besides, if the repetition rate of the signal is greater than characteristic inverse time of temperature equalization, $\frac{1}{F} << \tau_T$, then the temperature variation $\delta T << <T> - T_0$, assuming $T(t) = <T> + \delta T$. That leads us to $nk\frac{dT}{dt} \approx \frac{dP}{dt} \approx \frac{p(t)}{\frac{3}{2}V} - nk\frac{\langle T\rangle - T_0}{\tau_T} = \frac{p(t) - \langle p(t)\rangle}{\frac{3}{2}V}$. In the case when $<p(t)> = 0.5 p_{max}$, we get $\left.\frac{dP}{dt}\right|_{\max} = \frac{p_{\max}}{3V}$. It corresponds to the case of black body calibration, when shutter area is equal to half of the total modulator area. Here, p_{max} is the black body radiative power at fully open aperture. Then, $\left.\frac{CdU}{dt}\right|_{\max} = \frac{p_{\max}}{3V}$, and

$$C = \frac{p_{\max}}{3V\left.\frac{dU}{dt}\right|_{\max}}. \tag{8}$$

The voltage-power characteristic of the OAD, i. e. its optical sensitivity R, is known from measurement with reference black body, and the response for the described calibration conditions may be approximated with sine wave $U(t) = A \cdot \sin(wt)$ (where $w = 2\pi F$, $R = \frac{2A}{p_{\max}}$). That leads us to $\left.\frac{dU}{dt}\right|_{\max} = Aw = 2\pi AF = Rp_{\max}\pi F$. Taking into account (8), we get

$$C = \frac{1}{3\pi VRF}, \tag{9}$$

where F and its corresponding R values are obtained from voltage-power characteristic, so that $F >> \tau_T^{-1}$.

After initial estimation of the parameter set, the parameters are refined using reference calibration curves. However, the refining procedure should be somewhat different from the previous case. It's advisable to reconstruct several signal shapes at various frequencies, e. g. 1, 2 and 5 Hz. Time parameters, especially τ_P, are refined to achieve best fit for all three signals. Adequate accuracy may be obtained by using arithmetic mean τ_P for the three signals. Refinement of the parameter C is similar to the previous case, but with at least two reference black body signals (in the frequency range 15–25 Hz) instead of one, averaging the value. All responses $U(t)$ should be also averaged and smoothed.

When all calibration procedures are complete, arbitrary pulse shape $p(t)$ may be calculated using Eq. (7) with known parameters. Some examples of the reconstructed signal shapes are presented in Fig. 7.

Take a notice of the Fig. 7(c) showing a black body signal modulated by a pair of bandpass filters, which let through unequal bands of the black body spectrum. Calculated incident signal is a periodic sequence of a pair of bell-shaped pulses, completely consistent with expectations.

Measuring a shape of a single pulse is a particular sub-case of the case discussed in this section, assuming infinite repetition period and finite pulse length. Thus the Eqs. (6) and (7) can be modified, assuming $\alpha = 1$ (since xenon density in the chamber sub-volumes will completely equalize after an isolated pulse), and $P(t) = CU(t) + P_0$, since oscilloscope signal before and after the pulse is strictly zero. Examples of reconstructed single-pulse shapes are presented in Fig. 8.

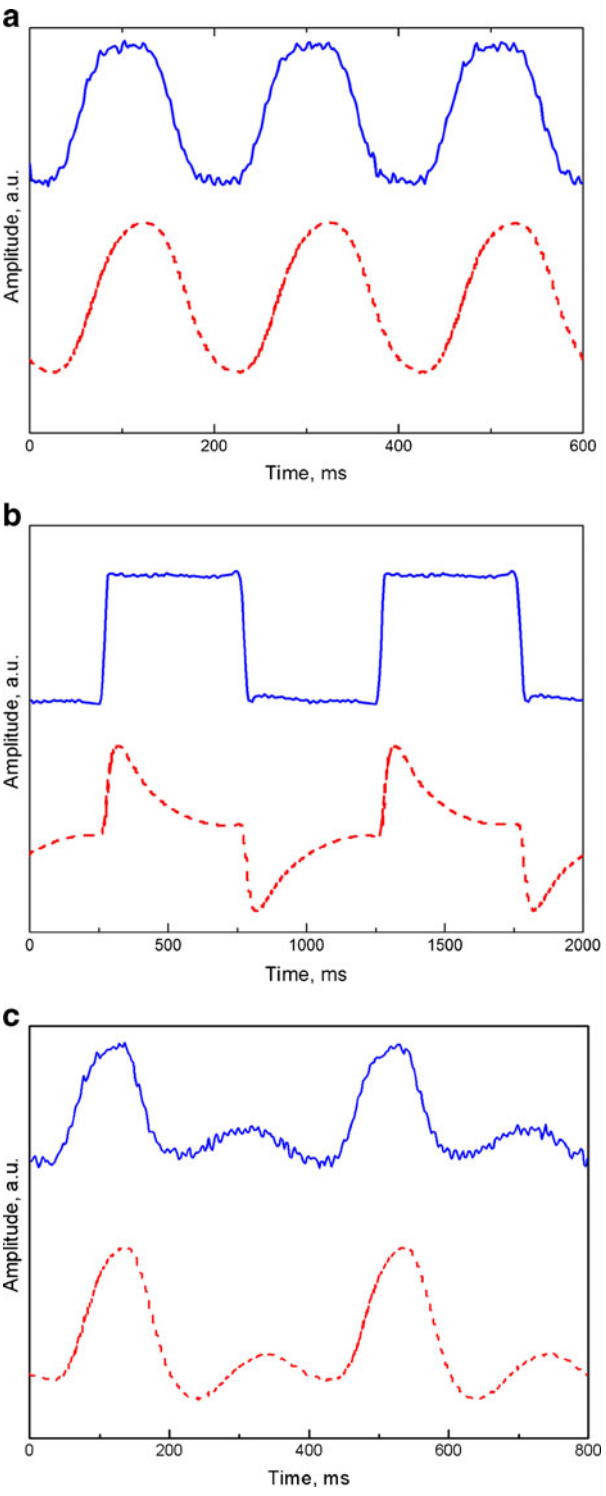

Fig. 7 OAD response vs time (dash) and corresponding calculated incident signal (solid). (**a**) – modulated black body signal, modulation frequency 5 Hz, (**b**) – meander 500+500 ms. (**c**) – black body signal modulated by a pair of rotating band-pass filters.

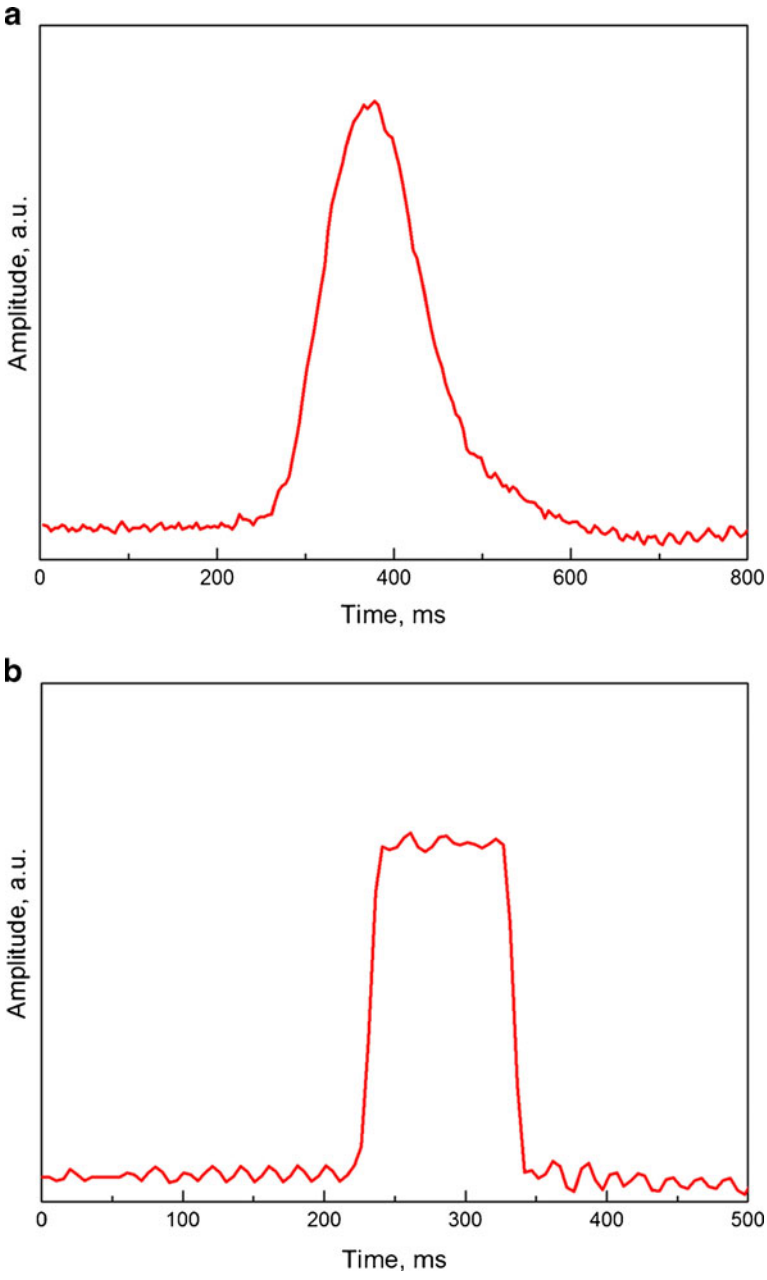

Fig. 8 (**a**) – 200 ms bell-shaped pulse. (**b**) – 100 ms rectangular pulse.

Characteristic instrument response curve *U(t)* is depicted in Fig. 9. Sharp rising and dropping regions correspond to heating and cooling with a change of density ($P>P_0$), whereas gradual increase region corresponds to density equalization ($P<P_0$). It should be noted that any damped pulse train is a special case of a single pulse and may be reconstructed the same way.

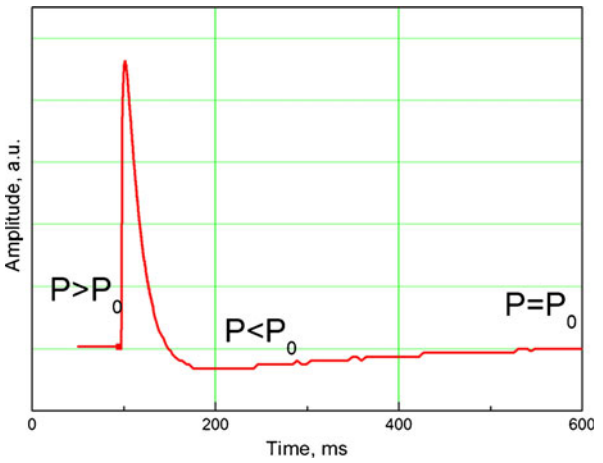

Fig. 9 Characteristic OAD response to the single pulse.

For calculation of energy W per ultra-short impulse (with duration about nano-, pico-seconds *etc*) we may use Eq. (7) with 2nd and 3rd terms being neglected in right part, because $\tau_P, \tau_t >> t_{pulse}$, where t_{pulse} is impulse duration. Therefore

$$W = \int_{before\,pulse}^{after\,pulse} p(t)dt = \frac{3}{2} VP(t)|_{before\,pulse}^{after\,pulse} = \frac{3}{2} VC\Delta U \tag{10}$$

where ΔU is the amplitude of signal related to pulse duration.

Finally, let us discuss lower limit of pulse duration of 0.5 ms. Left part of Fig. 10 shows that right tail of the reconstructed single pulse contains a train of periodic oscillations with a period of 0.5 ms. Right part of Fig. 10 shows the corresponding part of the responce in more detail (with inverted pulse).

Most probable cause of such oscillations is either elastic vibrations of the films, or voltage oscillations in the electronic circuits of the instrument. These oscillations are steadily reproduced. It is clear that any pulse shorter than the period of these oscillations will not

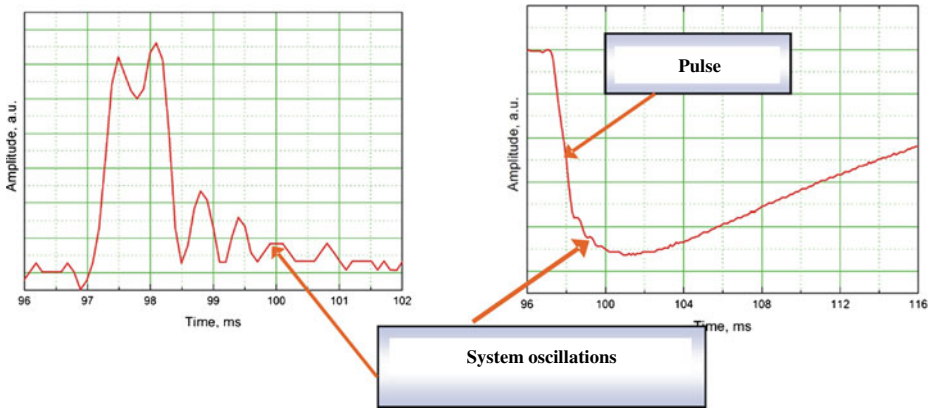

Fig. 10 Calculated signal shape and instrument response.

be seen against such a background. Therefore, one of the ways of further improvement of the OAD performance would be elimination of these oscillations.

3 Conclusions

In this paper the key physical processes within the active area of an optoacoustic detector are discussed. Pioneering mathematical model of an OAD is presented. This model is based on characterization of thermodynamic processes within the active area of the instrument. On the basis of the proposed model, the method has been developed to measure a shape of a periodic IR/THz/RF pulse exceeding 0.5 ms duration at repetition rate ranging from zero to several hundred Hz. High rate limit is dependent on signal/noise ratio of the external signal rather than OAD characteristics.

To measure the time dependence of incident power *p(t)*, a set of instrument-specific parameters must be evaluated using developed calibration procedure. Calibration procedure requires a source of a periodic signal with known power, as well as a source of a periodic signal with constant power regions (zero for example).

Broadening of the model to other types of gas-based opto- or photo-acoustic detectors after some adaptation (for example, account of resonant properties of the device) is possible, but there is the subject of special work that should also include experiments with other detector types.

Acknowledgement This work was supported by the Russian Foundation for Assistance to Small Innovative Enterprises (FASIE).

References

1. D. Ball, Spectroscopy, V. 21, Issue 9, 2006, pp 14–16.
2. A. Rosencwaig, *Photoacoustics and Photoacoustic Spectroscopy* (R.E. Krieger Publishing Company, Malabar, Florida, 1980).
3. A. Rosencwaig and A. Gersho, Science 190, 556 (1975).
4. L.-G. Rosengren, Appl. opt.,V14, N8, (1975) pp1960-1976
5. G. Busse, D. Herboeck, Appl. opt., V18, N23 (1979) pp3959-3961
6. S. Firebaugh, K. Jensen, and Martin A. Schmidt, J. MEMs, V10, N2 (2001) pp232-237
7. G. Busse, Appl. opt., V. 21, N. 1 (1982) pp107-110
8. M. J. Kavaya, "Optoacoustic detection employing Stark voltage modulation and Stark polarization modulation", PhD thesis, Caltech, Pasadena, California, 1982
9. E. L. Kerr and J. G. Atwood, Appl. Opt. 7, 915 (1968).
10. J. Gupta and R. Sachdev, Appl. Phys. Lett. 36 (12). (1980) pp 960–962
11. D. Leslie, G. Trusty, Appl. Opt., V20, N11 (1981) pp1941-1947
12. V. Andreev, V. Vdovin, Izv. VUZov, radiophisica, V. XLVIII, № 10–11, pp1-6
13. M. J. E. Golay, Rev. Sci. Instr., 18, 347 (1947)
14. M. J. E. Golay, Rev. Sci. Instr., 20, 816 (1949)
15. http://www.npl.co.uk/electromagnetics/terahertz/research/
16. P. Kaufmann, R. Marcon *etc*, J. Microwaves, Optoelectronics and Electromagnetic Applications, V10, N1 (2011), pp288-294
17. J. Cleary, C. Fredricksen *etc*, Proc. SPIE, V6472 64720E1-12 (2007)
18. http://www.m2lasers.com
19. S. Gavrish, V. Gmaev, A. Kobzar, V. Loginov, Appl. Phys, N1, pp53-59, 2009